

# Charge-state distributions after radiative capture of helium nuclei by a carbon beam

J. Zylberberg<sup>a,b</sup>, D. Hutcheon<sup>a,\*</sup>, L. Buchmann<sup>a</sup>, J. Caggiano<sup>a</sup>, W.R. Hannes<sup>c</sup>,  
A. Hussein<sup>d</sup>, E. O'Connor<sup>a,e</sup>, D. Ottewell<sup>a</sup>, J. Pearson<sup>f</sup>, C. Ruiz<sup>a,b</sup>,  
G. Ruprecht<sup>a</sup>, M. Trinczek<sup>a</sup>, C. Vockenhuber<sup>a,b</sup>

<sup>a</sup> TRIUMF, Science Division, 4004 Wesbrook Mall, Vancouver, BC, Canada V6T 2A3

<sup>b</sup> Simon Fraser University, Burnaby, BC, Canada

<sup>c</sup> University of Konstanz, Konstanz, Germany

<sup>d</sup> University of Northern BC, Prince George, BC, Canada

<sup>e</sup> University of PEI, Charlottetown, PE, Canada

<sup>f</sup> McMaster University, Hamilton, ON, Canada

Received 27 July 2006; received in revised form 13 September 2006

Available online 16 November 2006

## Abstract

We present new measurements of the charge-state distribution (CSD) of a 1.068 MeV/u C beam in He and of the  $6^+ : 5^+$  charge-state population ratio in the recoils of the  $^{12}\text{C}(\alpha, \gamma)^{16}\text{O}$  reaction, both measured at the DRAGON recoil mass spectrometer. A computer simulation to model the CSD of both beam and recoil particles in inverse-kinematics experiments is compared to data from this work and from previous work at ERNA. The simulation provides good agreement with both data sets. The results suggest that, for this fusion reaction on the  $J^\pi = 4^+$  resonance at  $E_{\text{beam}} = 1.064$  MeV/u, immediately after fusion, the recoil ions contain only the nucleons and not the electrons of the target He atom.

© 2006 Elsevier B.V. All rights reserved.

PACS: 55.20.Hv; 34.50.Fa; 25.40.Lw

Keywords: Ion charges; Gas target; Radiative capture; Fusion reaction; Charge state distribution

## 1. Introduction

Electromagnetic recoil mass spectrometers, such as DRAGON [1,2], at the ISAC facility at TRIUMF in Vancouver, Canada and ERNA [3–5], at the Dynamitron Tandem Laboratory of the Ruhr-Universität in Bochum, Germany, are used to investigate astrophysically important nuclear reactions in inverse kinematics. In such apparatus, only one charge state of the heavy recoil product can be transmitted for a given separator setting. Thus, in order to accurately determine the yield from a reaction, the

charge-state distribution (CSD) of the recoils must be known. For an extended gas target this poses a challenge since the CSD of the recoils will depend on where in the target they were created: those created toward the upstream end pass through the most gas, so they are the most likely to reach an equilibrium CSD [6]. This complication is compounded by the fact that the number of recoils produced per unit distance may change as the beam particles move through the target (as their energy changes, so may the fusion cross-section).

Previous studies at DRAGON [7,8], ERNA [6] and elsewhere [9,10] have measured the CSD of various beams passing through different gas targets. Of these studies, only one [6] has measured the CSD of the recoils. The Schürmann et al. work [6] investigated the CSD of recoils from

\* Corresponding author. Tel.: +1 604 222 1047x6474; fax: +1 604 222 1074.

E-mail address: [hutcheon@triumf.ca](mailto:hutcheon@triumf.ca) (D. Hutcheon).

the  $^{12}\text{C}(\alpha, \gamma)^{16}\text{O}$  reaction. Along with their measurements, Schürmann et al. also tried to predict the CSD of the recoils produced in the He target. Their model assumed that, in the fusion reaction, the charge on the recoil ion was the same as the charge on the beam ion (i.e. the recoil contains both the electrons and the nucleons of the target particle). This model was in stark disagreement with their data, suggesting that the above assumption may be faulty.

In this work, we present our measurements of the CSD of the beam and the  $F_6/F_5$  ratio (where  $F_q$  denotes the fraction of particles in charge-state  $q$ ) in the recoils of the  $^{12}\text{C}(\alpha, \gamma)^{16}\text{O}$  reaction on the  $J^\pi = 4^+$  resonance at  $E_{\text{beam}} = 1.064$  MeV/u ( $E_{\text{cm}} = 3.19$  MeV), along with a computer simulation (CSDsim) that models the changing CSD of beam and recoil particles as they move through the target. The simulation is then applied to this reaction and the results are compared to experimental data from DRAGON (this work) and ERNA [6] in order to determine how the ion charge changes during the fusion reaction.

## 2. Experimental procedure

### 2.1. Beam charge-state distribution

Charge-state distributions of carbon ions were measured after a 1.068 MeV/u beam of  $^{12}\text{C}$  in the  $3^+$  charge-state passed through different thicknesses of He gas. The He gas was contained in the windowless gas target system of DRAGON. As described in [1,2,11], it consists of a central gas cell having small entrance and exit apertures and a series of differential pumping stages. For hydrogen gas and apertures of 6 and 8 mm, the effective length of the target has been determined to be  $123 \pm 4$  mm [11]. The measurements described here were made with apertures of 4 and 10 mm diameter, which had a combined cross-sectional area 16% larger than that for the 6/8 mm case.

The total thickness of gas traversed by the beam is assumed to be proportional to the central pressure in the cell for a given aperture pair and type of gas. Support for this assumption comes from measurements of beam energy loss for various pressures from 0.4 to 4.6 Torr: the rms deviation from linearity was less than 5% of the energy loss at 4.6 Torr. The apertures and gas type can affect the pressure in the target region outside the central cell (including the pumping tubes leading to the next stages of differential pumping), relative to the pressure in the central cell. This ratio,  $f$ , is the principal factor that determines the amount ( $13 \pm 4$  mm) by which the effective length of the target system exceeds the physical length of the central cell. (Less important is a possible change of profile in the short region of rapid pressure drop near the cell apertures.) For the same gas type, the 16% increase in summed aperture areas is expected to increase their conductance by 16% [12] and therefore increase  $f$  by 16% also. Measurement of  $f$  for He gas gave a result that was  $16 \pm 9\%$  lower than  $f$  for  $\text{H}_2$  gas for the same aperture set. We have assumed the

effective length for the He measurements to be 123 mm with an uncertainty of 6 mm. The target temperature was 300 K, with variation of less than 1%, leading to a calculated  $3.96 \times 10^{17}$  atoms/cm<sup>2</sup> target thickness for a central cell pressure of 1 Torr.

Beam currents were measured in biased Faraday cups (FC) at three locations (Fig. 1): (1) FC4 at a beam focus 3.5 m upstream of the gas target, (2) FC1 downstream of the gas target and in front of the first magnetic dipole of the DRAGON separator and (3) FCCH after slits at a focus immediately after the first magnetic dipole. Accordingly, FC4 measured the current of incident  $3^+$  beam, FC1 measured the beam transmitted through the gas cell summed over all charge-states and FCCH measured the transmitted beam current for one selected charge-state.

Beam currents were measured for central cell pressures of 0.25, 0.50, 1.0 and 3.96 Torr. At the two middle pressures, FCCH currents were measured for selected charge-states  $4^+$ ,  $5^+$  and  $6^+$ , while at the other two pressures only charge-states  $5^+$  and  $6^+$  were observed. By comparison of the currents in FC4, FC1 and FCCH, it was possible to deduce the beam transmission (80–85%), fractions for the measured charge-states and at the highest pressure to deduce  $F_4$ .  $F_3$  could not be measured directly because the magnetic dipole did not have enough bending power for C ions of 1.068 MeV/u in that charge-state.

### 2.2. Recoil charge-state distribution

The full DRAGON system of gas target, gamma-detection (bismuth germanate scintillators: BGO) array, mass separator and recoil particle detector was used to detect the gamma rays and  $^{16}\text{O}$  recoil ions which result from radiative alpha capture by  $^{12}\text{C}$  into the  $J^\pi = 4^+$  resonance at  $E_{\text{cm}} = 3.19$  MeV. The BGO array had a hardware threshold set to trigger upon detection of either or both members of the 3.5 and 6.9 MeV cascade, giving a trigger efficiency of approximately 70%. Energy of the recoil ions was registered in a double-sided silicon-strip detector (DSSSD) at the end of the separator. The standard (for proton capture experiments) downstream pumping tubes of the gas target were replaced by a set having a nominal acceptance half-angle of 25 mrad. Yields were measured as the number of BGO–DSSSD coincidences, normalized to counts in a

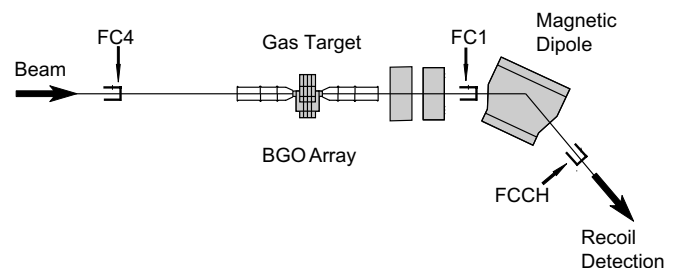


Fig. 1. Diagram of the relevant components of the DRAGON apparatus for the beam CSD measurements. FC denotes a Faraday cup.

Si-surface barrier detector which counted alpha particles from elastic scattering of the beam in the He gas target. The coincidence requirement ensured a background-free signal, even at the lowest gas pressures.

We emphasize that to obtain an unbiased measure of the ratio  $F_6/F_5$  it is not essential to understand exact values of efficiency and normalization, but only the extent to which they differ between the two charge states. In an electromagnetic separator with ion transport through vacuum, identical values for field strength divided by the ion charge produce identical ion trajectories. DRAGON's separator magnets operate far from saturation so magnetic field profiles are not expected to change between the tune for  $5^+$  ions and that of  $6^+$  ions (see Table 2 of [2]). A potential source of bias in measuring  $F_6/F_5$  arises if the production of  $5^+$  recoils is mainly in the upstream half of the target and of  $6^+$  recoils is mainly in the downstream half of the target (say), while the detection efficiency is not symmetric about the mid-point ( $z = 0$ ) of the gas cell. This is most likely to be a concern at 0.25 Torr, where the mean free path for the C beam to change to  $q = 4^+$  from the initial  $3^+$  is roughly equal to the length of the target cell. The desired symmetry is present for two of the principal factors that determine the overall efficiency: the gamma-ray detection efficiency is nearly symmetric between  $z = -8$  cm and  $z = +8$  cm where  $>95\%$  of the target gas is located (see Fig. 6 of [13]); the separator acceptance depends upon the apparent beam spot size when recoil trajectories are projected to  $z = 0$ , but the effect is the same for upstream and downstream reaction points of the same  $|z|$ , because of the azimuthal symmetry of the capture reaction. The acceptance manifestly is different for reactions taking place upstream of the upstream cell aperture compared to reactions downstream of the downstream aperture; this matters only for a part of the range in azimuthal angles for reactions well off the beam axis or well upstream, where less than 5% of the gas is found, however. At higher pressures the mean free path between charge-changing collisions of beam ions is much shorter and the  $z$ -dependence of beam CSD is correspondingly less important.

The beam energy was adjusted to give maximum yield of recoil ions at a target pressure of 3.96 Torr. The relative yields of  $5^+$  and  $6^+$  recoil ions were measured at this pressure and at 0.25, 0.50 and 1.0 Torr without any further adjustment of beam energy. The  $4^+$  recoil yields could not be measured because the DSSSD would have been swamped by a low-energy tail of the  $^{12}\text{C}$  beam in the  $3^+$  charge-state, which has the same mass/charge ratio and therefore could not be eliminated by the separator.

### 3. Experimental results and discussion

#### 3.1. Charge-state distribution of C beam in He

Table 1 shows our results for the CSD of a  $\text{C}^{3+}$  beam in a He target at 12.82 MeV, while Table 2 shows previously unpublished DRAGON results [8] for the CSD of a  $\text{C}^{3+}$

Table 1

Measured charge-state distributions of 12.82 MeV  $\text{C}^{3+}$  beam in He target

Pressure (Torr)	$F_4$	$F_5$	$F_6$
3.96	$0.17 \pm 0.03$	$0.54 \pm 0.03$	$0.292 \pm 0.015$
1.0	$0.41 \pm 0.02$	$0.50 \pm 0.02$	$0.084 \pm 0.004$
0.5	$0.57 \pm 0.03$	$0.274 \pm 0.014$	$0.021 \pm 0.0011$
0.25	Not measured	$0.10 \pm 0.005$	$0.005 \pm 0.0003$

Table 2

Measured charge-state distributions of 12.0 MeV  $\text{C}^{3+}$  beam in He target; previously unpublished data from [8]

Pressure (Torr)	$F_4$	$F_5$	$F_6$
5.35	0.140	0.583	0.277
3.99	0.156	0.588	0.257
3.09	0.180	0.589	0.231
2.08	0.197	0.613	0.191
1.26	0.286	0.517	0.197
0.72	0.557	0.407	0.037

beam in a He target at 12.0 MeV. The uncertainties in our data come from a 5% uncertainty in the transmission value and a 10 epA uncertainty on each FC measurement, which were added in quadrature. It should be noted that, in our data, there is a 5% scale uncertainty in target thickness associated with the uncertainty in effective target length.

Our value for  $F_6$  after a 3.96 Torr He target is in excellent agreement with a previous polynomial fit for  $F_6(P, E)$  [8]. This fit is valid only for DRAGON target pressures above 3 Torr, so it cannot be used to verify the lower-pressure data points. Nevertheless, this agreement confirms the accuracy of our measurement.

The main differences between the data sets in Tables 1 and 2 are that they were measured at (slightly) different energies and that the analysis used to extract the data in Table 2 assumed that the population of the  $3^+$  charge-state was zero, while our analysis made no such assumption. Despite these discrepancies, there is still useful information in Table 2: the equilibrium CSD is reached with a DRAGON target pressure of roughly 3 Torr. Since these data points were collected at an energy similar to the 12.82 MeV beam energy used in the current study, it suggests that, at the present energy as well, equilibrium is likely reached near that 3 Torr pressure.

#### 3.2. $F_6/F_5$ ratio in the recoils of $^{12}\text{C}(\alpha, \gamma)^{16}\text{O}$

The measured  $F_6/F_5$  ratios in the recoils at several different pressures are shown in Table 3. The uncertainties in this data come from the relative statistical uncertainties in the number of counts for the  $5^+$  and  $6^+$  states, which were added in quadrature.

The data set shows a non-linear variation in the  $F_6/F_5$  ratio over the pressure range studied. This variation provides strong motivation for the development of the CSD-sim code, since an accurate knowledge of the recoil CSD is needed in order to properly analyze experimental data.

Table 3  
Measured  $F_6/F_5$  ratio in the recoils of  $^{12}\text{C}(\alpha, \gamma)^{16}\text{O}$  on the  $J^\pi = 4^+$  resonance

Pressure (Torr)	$F_6/F_5$
3.96	$0.68 \pm 0.04$
1.0	$0.96 \pm 0.08$
0.5	$0.92 \pm 0.10$
0.25	$0.82 \pm 0.10$

The mechanism behind this variation is discussed below, in Section 5.

There is no other data with which to compare these results, as Schürmann et al. did not report  $F_5$  in the recoils from their experiment.

## 4. Simulation

### 4.1. CSDsim code

The CSDsim code was written in C programming language and is essentially a numerical integrator (with a few extra features: to be discussed in this section) that solves the set of coupled differential equations (1) which describes the changing CSD of a group of particles traveling through matter [7]. Since the energy losses are quite low in the inverse-kinematics experiments that CSDsim models, the charge-changing cross-sections are assumed to be constant throughout the simulation

$$\frac{dF_q}{dx} = \sum_{q', q' \neq q} (F_{q'} \sigma_{q', q} - F_q \sigma_{q, q'}). \quad (1)$$

Eq. (1) is bound by condition (2) [7].

$$\sum_q F_q = 1. \quad (2)$$

For each slice of the target (a user-defined variable:  $10^{13}$  atoms/cm<sup>2</sup> was used for the simulations discussed here), the program recalculates the CSD of the beam and (existing) recoils using Eq. (1). It then calculates the energy of the beam, assuming linear energy loss (which is suitable for the relatively small energy losses being discussed here), using  $dE/dx$  values from the SRIM2003 Tables [14]. CSDsim then calculates an updated fusion cross-section from a Breit–Wigner-type Eq. (3), which allows it to model the changing number of recoils produced in each slice of the target

$$\sigma_{\text{fusion}} = \sigma_{\text{max}} \left( 1 + \left( \frac{E_{\text{beam}} - E_{\text{resonance}}}{\frac{\Gamma_{\text{total}}}{2}} \right)^2 \right)^{-1}. \quad (3)$$

The CSD of the recoils being created is then calculated by multiplying the beam CSD matrix by a matrix which describes the probability of creating a recoil of a given charge for each possible beam charge-state (charge-probability or CP matrix). As an example, the general CP matrix for the  $^4\text{He}(^3\text{H}, \gamma)^7\text{Li}$  reaction with a  $^4\text{He}$  beam is

$$\text{CP matrix} = \begin{pmatrix} P_{0,0} & P_{1,0} & P_{2,0} \\ P_{0,1} & P_{1,1} & P_{2,1} \\ P_{0,2} & P_{1,2} & P_{2,2} \\ P_{0,3} & P_{1,3} & P_{2,3} \end{pmatrix},$$

where  $P_{a,b}$  represents the probability of creating a recoil of charge  $b$  from a beam ion of charge  $a$ .

The resultant “new” recoil CSD is then multiplied by the number of recoils to be added in the slice ( $dx \cdot \sigma_{\text{fusion}}$ ) and added to the existing recoil CSD matrix (which has been multiplied by the number of existing recoils). Finally, CSDsim normalizes the recoil CSD matrix so that Eq. (2) is obeyed.

For each slice of the target, CSDsim also calculates the energy of the recoils being produced (which is assumed to be constant over all recoils). By assuming that the momentum of the recoils is roughly the same as that of the beam particles, the energy of the recoils is calculated to be

$$E_{\text{recoil}} = E_{\text{beam}} \frac{m_{\text{beam}}}{m_{\text{recoil}}}, \quad (4)$$

where  $m_{\text{beam}}$  and  $m_{\text{recoil}}$  are the masses of the beam and recoil particles, respectively.

CSDsim outputs the beam and recoil CSD, the average energy of the beam and recoil particles and the total number of recoils created in the last cycle after a user-defined interval (once per 100 slices for the simulations discussed here). The resultant data files can be used in acceptance simulations, where the geometric location of recoil production is important and in analyzing data, where the CSD of the beam and recoils are important.

### 4.2. Simulation procedure

To start, we fit a set of charge-changing cross-sections (CCCS’s) to experimental data for a C beam in He at 12.82 MeV (from this work) and for an O beam in He at 9.6 MeV [6] [which is the energy of the oxygen recoils, according to Eq. (4)]. In each case, this was done by first finding a nominal CCCS set and then using a least-squares algorithm to find the “best” CCCS’s and the uncertainties therein.

The generated CCCS sets account for single-electron losses and gains only, as the CCCS’s for multiple-electron processes in He gas are known to be quite small [9].

The nominal CCCS sets were found by first setting the ratios of the CCCS’s to be such that the correct equilibrium CSD was reached, i.e. Eq. (5) and then scaling the individual  $\sigma_{q,q'}$ ,  $\sigma_{q',q}$  pairs together (multiplying them both by the same value) until the charge-state populations changed at a rate that agreed roughly with the experimental data.

$$\frac{\sigma_{q,q'}}{\sigma_{q',q}} = \frac{F_{q'}}{F_q}. \quad (5)$$

Once these nominal CCCS’s were found, we iteratively recalculated the resultant CSD, each time perturbing one of the CCCS’s by  $\pm 10\%$  from the nominal value. The  $\chi^2$

value for each of these CSD's (as compared with the experimental data in which the uncertainties were normalized so that  $\chi^2$  per degree of freedom was 1) was then calculated. Next, we fit a parabola to the  $\chi^2$  vs  $\sigma_{q,q'}$  distribution, which allowed us to determine the best CCCS and the uncertainty on the cross-section (the deviation from the “best” CCCS for which the  $\chi^2$  value increased by 1). In each case, this process was repeated twice in order to ensure the reliability of the CCCS's.

In cases where the equilibrium ratio between states  $q$  and  $q + 1$  was known, only the electron loss CCCS (i.e.  $\sigma_{q,q+1}$ ) was found in the above manner and the corresponding electron capture CCCS ( $\sigma_{q+1,q}$ ) was determined by Eq. (5). In these instances, the estimated error on the electron capture CCCS was the result of adding, in quadrature, the error on the electron loss CCCS and the uncertainty in the equilibrium charge-state population ratio.

Once we had determined the CCCS's, we investigated how changing the CP matrix (which describes the electron loss/capture behavior during fusion) affected the behavior of the model by comparing CSDsim predictions using different CP matrices to data for  $F_6$  [6] and the  $F_6/F_5$  ratio in the recoils of  $^{12}\text{C}(\alpha,\gamma)^{16}\text{O}$ . The CP matrices studied reflected several different physically plausible behaviors:

- (1) The recoil Picks Up both electrons (PU2e) of the target particle, thus  $q_{\text{recoil}} = q_{\text{beam}}$  (this is the assumption made in [6]).
- (2) The recoil Picks Up none of the electrons (PU0e) from the target, thus  $q_{\text{recoil}} = q_{\text{beam}} + 2$ .
- (3) The ratios between the Charge-State Probabilities are the same as the ratios between the Equilibrium Fractions (CSPEF) of the recoils.
- (4) The Charge-State Probabilities are such that they Maximize production in the  $5^+$  State (CSPM5S) (which has the largest population at equilibrium [6]).
- (5) The charge-state probabilities are a mixture PU2e and PU0e behavior.

## 5. Simulation results and discussion

### 5.1. Charge-changing cross-sections

The data for CSD as a function of target thickness for a  $\text{C}^{3+}$  beam at 12.82 MeV (from this work) and an  $\text{O}^{3+}$  beam at 9.6 MeV (from ref [6]) in a He target are shown in Figs. 2 and 3, respectively. Also shown in these figures are the CSDsim fits to the data. In both cases, the agreement between the CSDsim fit and the experimental data confirms the validity of our model.

Our CCCS's are listed in Tables 4 and 5 along with CCCS's from [9]. Direct comparison of these CCCS sets is difficult since these CCCS sets are for different energies and there is strong nonlinearity in the velocity (energy) dependence of the CCCS's [15]. However, a comparison between our CCCS's for a 12.82 MeV C beam in He and

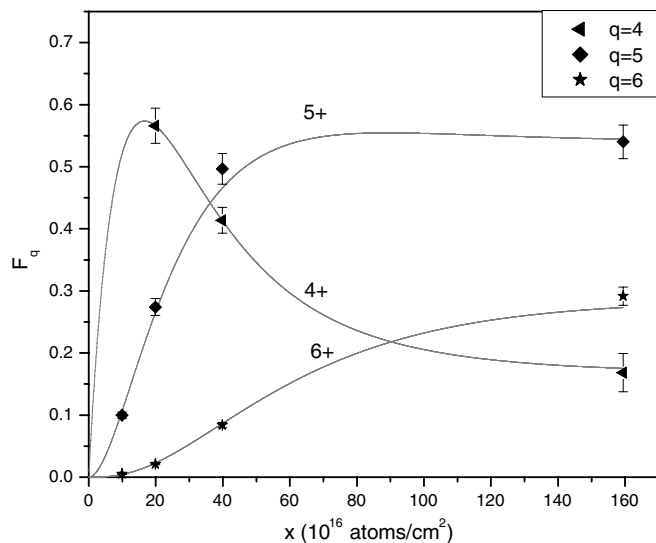


Fig. 2. Charge-state fractions as a function of target thickness for a 12.82 MeV  $\text{C}^{3+}$  beam in He. The solid lines are CSDsim predictions using the fitted cross-sections (see text).

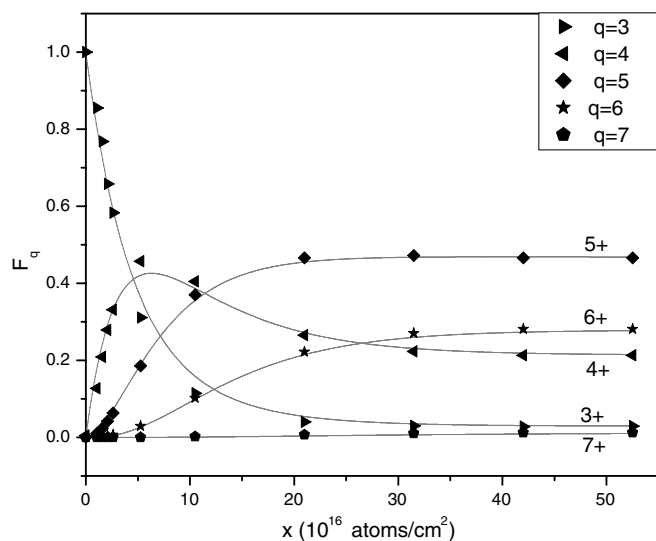


Fig. 3. Charge-state fractions as a function of target thickness for an 9.6 MeV  $\text{O}^{3+}$  beam in He. The solid lines are CSDsim predictions using the fitted cross-sections (see text). The data shown are results from [6].

those of Dillingham et al. (for a 12 MeV  $E_{\text{beam}}$ ) shows that, in all cases, the Dillingham et al. CCCS's are roughly 70–80% as large as ours, which is reasonably good agreement between these CCCS sets. Comparison between our CCCS's and those of Dillingham et al. for a 13.6 MeV  $E_{\text{beam}}$  are not as good: the Dillingham et al. CCCS's range from 30% to 70% of ours.

### 5.2. Recoil charge-state distributions and charge-probability matrices

Fig. 4 shows the  $F_6/F_5$  ratio in the recoils for simulations with various CP matrices (representing behaviors 1–5, see

Table 4  
Charge-changing cross-sections for C in He, in  $10^{-18}$  cm<sup>2</sup>/atom; comparison between those developed in this work and those listed in [9]

CCCS	Dillingham 12 MeV	This work (12.82 MeV)	Dillingham 13.58 MeV
$\sigma_{6,5}$	$1.77 \pm 0.17$	$2.2 \pm 0.2$	$0.813 \pm 0.046$
$\sigma_{5,6}$	$0.723 \pm 0.048$	$1.14 \pm 0.06$	$0.823 \pm 0.044$
$\sigma_{5,4}$	$0.868 \pm 0.037$	$1.1 \pm 0.2$	$0.361 \pm 0.022$
$\sigma_{4,5}$	None listed	$3.5 \pm 0.1$	None listed
$\sigma_{4,3}$	None listed	$0.4 \pm 0.5$	None listed
$\sigma_{3,4}$	None listed	$10.3 \pm 0.4$	None listed

Table 5  
Charge-changing cross-sections for O in He, in  $10^{-18}$  cm<sup>2</sup>/atom; comparison between those developed in this work and those listed in [9]

CCCS	Dillingham 9 MeV	This work (9.6 MeV)	Dillingham 16 MeV
$\sigma_{7,6}$	$24.0 \pm 1.2$	$6 \pm 3$	$2.48 \pm 0.07$
$\sigma_{6,7}$	None listed	$0.25 \pm 0.12$	None listed
$\sigma_{6,5}$	None listed	$13 \pm 3$	None listed
$\sigma_{5,6}$	None listed	$7.8 \pm 1.4$	None listed
$\sigma_{5,4}$	None listed	$7.3 \pm 0.8$	None listed
$\sigma_{4,5}$	None listed	$16 \pm 1$	None listed
$\sigma_{4,3}$	None listed	$2.9 \pm 0.3$	None listed
$\sigma_{3,4}$	None listed	$20.9 \pm 0.5$	None listed

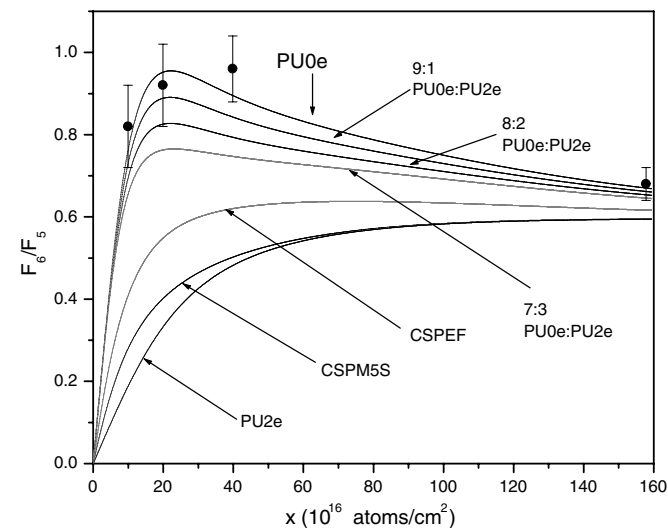


Fig. 4.  $F_6/F_5$  ratio in the recoils of  $^{12}\text{C}(\alpha, \gamma)^{16}\text{O}$  as a function of target thickness. The solid lines are CSDsim predictions using different recoil charge-probability matrices (see text).

Simulation Procedure section for details), along with experimental data from this work. The agreement between the simulation and the experiment is quite good for a PU0e CP matrix (see Simulation Procedure section for details) and becomes progressively worse as the CP matrix is modified to include more of the PU2e behavior. Similarly, CP matrices which reflect PU2e, CSPEF and CSPM5S behavior are all in strong disagreement with the data. This suggests that, in the  $^{12}\text{C}(\alpha, \gamma)^{16}\text{O}$  reaction (at 1.06 MeV/u in

the lab frame), immediately after fusion, the recoils do not contain the electrons of the target particle.

Similarly, Fig. 5 shows both data (from [6]) and simulation results (CSDsim and the simulation used in [6]) for  $F_6$  in the recoils. The results for a simulation with PU2e behavior (the assumption made by Schürmann et al.) agree qualitatively with the prediction made by Schürmann et al. and both of these predictions fail to match the data. However, as in the above case of comparison with our results, the simulation with PU0e behavior is in much better agreement with the data. Unlike the above case, however, the CSDsim predictions with PU0e behavior still do not provide good agreement with this data set.

In an attempt to improve the agreement between the CSDsim predictions and the Schürmann et al. data, simulations were performed in which the PU0e behavior was modified so that Li-like ( $\text{C}^{3+}$ ) beam ions form a mixture of Li-like ( $\text{O}^{5+}$ ) and He-like ( $\text{O}^{6+}$ ) species in the fusion reaction (in addition to not gaining any electrons (PU0e behavior) during the fusion reaction, we allowed for the possibility that some may be lost). As an example, the CP matrix for PU0e behavior, modified so that Li-like beam ions form 90% Li-like and 10% He-like recoils, is

$$M_{90:10} = \begin{pmatrix} 0 & 0 & 0 & 0 & 0 & 0 & 0 \\ 0 & 0 & 0 & 0 & 0 & 0 & 0 \\ 1 & 0 & 0 & 0 & 0 & 0 & 0 \\ 0 & 1 & 0 & 0 & 0 & 0 & 0 \\ 0 & 0 & 1 & 0 & 0 & 0 & 0 \\ 0 & 0 & 0 & 0.9 & 0 & 0 & 0 \\ 0 & 0 & 0 & 0.1 & 1 & 0 & 0 \\ 0 & 0 & 0 & 0 & 0 & 1 & 0 \\ 0 & 0 & 0 & 0 & 0 & 0 & 1 \end{pmatrix}.$$

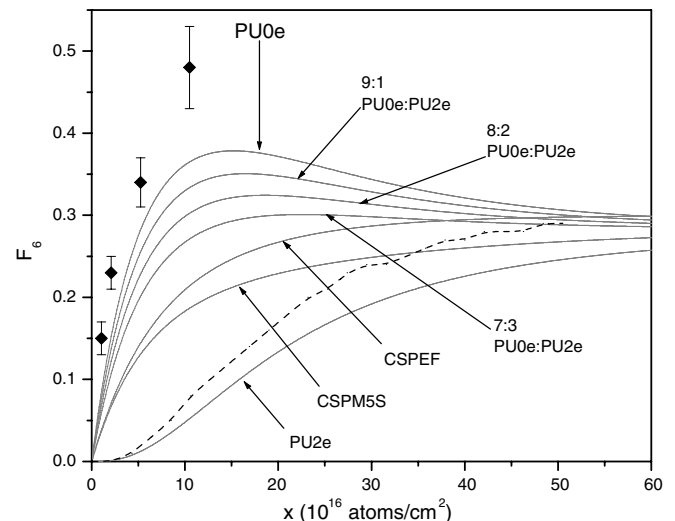


Fig. 5.  $F_6$  in the recoils of  $^{12}\text{C}(\alpha, \gamma)^{16}\text{O}$  as a function of target thickness. The solid lines are CSDsim predictions using different recoil charge-probability matrices (see text). The data shown are results from [6]. The dashed line is the result of the simulation used in [6].

The results of these simulations are shown alongside data from this work and from [6] in Figs. 6 and 7, respectively. All of the curves shown (which represent different Li-like:He-like O recoil ratios from Li-like C ions) are in good agreement with our data. However, for comparison with the Schürmann et al. data, this is not the case: the 90:10 Li-like:He-like recoil model is clearly the best.

The broad peak in the  $F_6/F_5$  ratio in the recoils can be understood by observing how the CSD of the carbon beam changes in the He target. In Fig. 2, it can be seen that there is a peak in the  $C^{4+}$  fraction at a depth of roughly  $1.7 \times 10^{17}$  atoms/cm<sup>2</sup>. This corresponds closely to the approximately  $2.2 \times 10^{17}$  atoms/cm<sup>2</sup> depth at which the  $F_6/F_5$  ratio is seen to peak. We have already seen that, at this depth, the majority of the recoils have a charge 2 greater than that on the beam ion. Thus, we can infer that the peak in the recoil  $F_6/F_5$  ratio comes from the increased  $C^{4+}$  charge-state fraction at that depth.

It should be noted that CSDsim shows low sensitivity to certain CP matrix elements. In particular  $P_{6,8}$  and  $P_{6,7}$  can be interchanged in the above matrix without noticeably changing the predicted recoil CSD. Similarly, a reduction in  $P_{5,7}$  (with a subsequent increase in  $P_{5,8}$ ) causes no noticeable change in the predicted CSD over the whole (0–1) range of possible values. This is because  $\sigma_{8,7} \gg \sigma_{7,8}$  (at 9 MeV [9]), thus any recoils produced in the  $8^+$  state quickly change to the  $7^+$  state. Furthermore, reductions in  $P_{5,7}$  (with subsequent increases in  $P_{5,6}$ ) do cause noticeable changes in the  $F_6$  and  $F_6/F_5$  predictions of CSDsim, but over the range of possible values, the predictions all agree equally well with the  $F_6/F_5$  data (from this work) and the  $F_6$  data from ERNA [6].

Gialanella et al. [16] have made related measurements with an 11 MeV  $^{12}\text{C}$  beam and a hydrogen gas target.

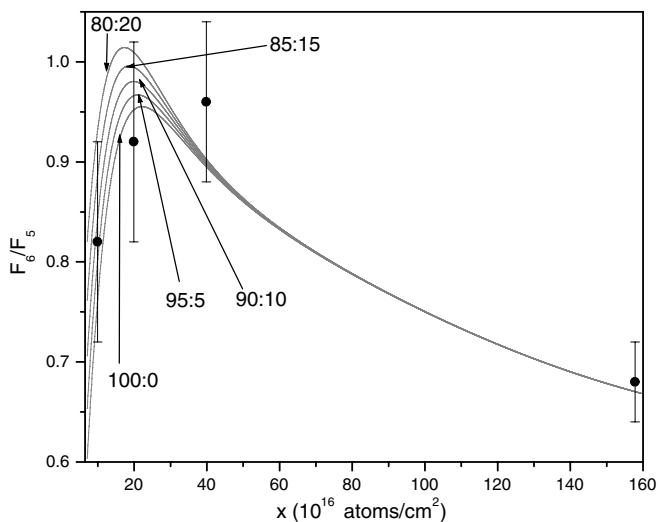


Fig. 6.  $F_6/F_5$  ratio in the recoils of  $^{12}\text{C}(\alpha, \gamma)^{16}\text{O}$  as a function of target thickness, where PU0e behavior with additional electron loss was modeled. The solid lines are CSDsim predictions which are labeled according to the ratio of Li-like:He-like recoils being created from Li-like beam ions.

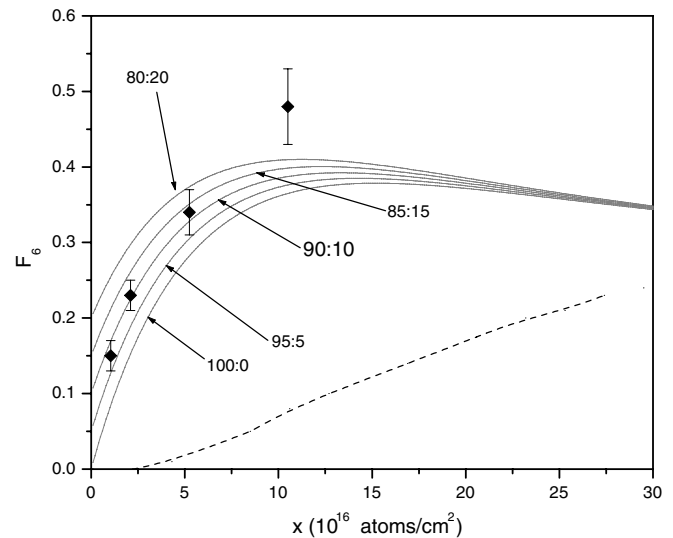


Fig. 7.  $F_6$  in the recoils of  $^{12}\text{C}(\alpha, \gamma)^{16}\text{O}$  as a function of target thickness, where PU0e behavior with additional electron loss was modeled. The solid lines are CSDsim predictions which are labeled according to the ratio of Li-like:He-like recoils being created from Li-like beam ions. The data shown are results from [6]. The dashed line is the result of the simulation used in [6].

For  $q = 5^+$  and  $q = 6^+$  beams they measured the yield  $Y_q$  of fully-stripped ( $7^+$ )  $^{13}\text{N}$  ions from the  $^{12}\text{C}(p, \gamma)^{13}\text{N}$  reaction and found  $Y_5/Y_6 = 0.77 \pm 0.07$ . They compared this to a model in which the  $^{13}\text{N}$  ions immediately after the capture reaction had the same charge as the incident C beam, then evolved towards the equilibrium CSD as they passed through the rest of the target: the model gave  $Y_5/Y_6 = 0.69 \pm 0.03$ . However, for their thick target ( $L_{\text{eff}} = 376$  mm, pressure 5 mbar) it is unrealistic to ignore the evolution of the  $^{12}\text{C}$  beam towards its equilibrium CSD. Including beam CSD evolution must push  $Y_5/Y_6$  much closer to 1.0. Insufficient data are available for a full CSDsim calculation, but gauging by the convergence of curves at the thick-target side of Fig. 5, it will be hard to distinguish PU0e from PU1e (or even a possible PU2e) in the data of [16].

Despite the limitations of our model, the results clearly show that electron capture and loss probabilities at the time of a nuclear capture reaction are different from the average probabilities experienced by ions which pass completely through a gas target. Capture reactions involve special conditions such as small (on the atomic scale) impact parameters and violent deceleration of the incident beam nucleus. However, it is not clear whether these features are the explanation for the difference in probabilities. Another open question is whether the behavior is specific to this beam energy (an “accident” due to atomic shell effects, say) or is a general feature of capture reactions.

In the absence of a proven, universal model for atomic charge changes during a capture reaction, special measures may be needed for certain radiative capture experiments with a gas target and recoil separator. Such cases include narrow resonances near the downstream end

of the target or reactions (broad resonances or direct capture) which occur throughout the entire length of the target. One approach, adopted at ERNA, is to add a post-stripper gas cell to bring all recoil ions to a known equilibrium charge-state distribution [6]. Another possibility is to use a thin stripper foil after the gas target, as successfully demonstrated in the  $^{40}\text{Ca}(\alpha, \gamma)^{44}\text{Ti}$  reaction at DRAGON [17].

In the limiting case of a very thick target, however, these precautions are unnecessary since the recoil CSD is the same as that of an oxygen beam passing through a He target; the recoil CSD is independent of the electron loss/capture behavior during fusion. For a reaction with a constant fusion cross-section, at a DRAGON target pressure of 4(8) Torr, making this thick-target assumption results in an overestimation of  $F_5$  by 12(5)% and an underestimation of  $F_6$  by 0.4(−0.2)% (when compared to the PU0e prediction). Similarly, at 4(8) Torr, the differences between the PU2e and PU0e predictions for  $F_5$  and  $F_6$  are 13(6)% and 1(0.5)%, respectively. Thus, another useful approach is to use a target of sufficient thickness that the uncertainty in the recoil CSD is minimized.

If none of the above methods can be used, then one can partition the experimental time, selecting recoils in the two or three most probable charge-states for separate yield measurements.

## 6. Conclusions

We have measured the CSD of a  $\text{C}^{3+}$  beam in a He target, as a function of target thickness, as well as the ratio of  $F_6/F_5$  in the recoils of the  $^{12}\text{C}(\alpha, \gamma)^{16}\text{O}$  reaction on the  $J^\pi = 4^+$  resonance.

The CSDsim code has been written and used to model this reaction in order to ascertain the change in the charge on a beam particle at the moment of the fusion reaction. The CSDsim code can provide good agreement with our results and those from [6]. Our data extended between target thicknesses of  $1 \times 10^{17}$  and  $16 \times 10^{17}$  atoms/cm<sup>2</sup>, while the data of [6] were in the range  $0.1\text{--}1.0 \times 10^{17}$  atoms/cm<sup>2</sup>. The best agreement with experiment comes when the model assumes that, at the moment of fusion, none of the electrons from the target He atom are captured. Furthermore, it appears that some of the recoils contain even fewer electrons than did the beam particles, indicating that some additional electrons may be lost during the fusion process. Our results were sensitive to the CSD of recoils produced from  $\alpha$  capture by  $\text{C}^{3+}$  and  $\text{C}^{4+}$  beam ions. More data is needed in order to develop a thorough understanding of the CSD following  $\alpha$  capture by  $\text{C}^{5+}$  or  $\text{C}^{6+}$  ions.

These results imply that it is, in some cases, necessary to measure the recoil CSD for inverse-kinematics experiments, because simplifying assumptions (like  $q_{\text{beam}} = q_{\text{recoil}}$ ) are not necessarily accurate.

This knowledge, along with the capabilities of the CSDsim code, are useful to those studying nuclear fusion reactions in inverse kinematics, like at DRAGON and ERNA.

## Acknowledgements

We are grateful to the Natural Sciences and Engineering Research Council of Canada for financial support. We would further like to thank Dr. D. Schürmann for providing us with numerical values for the data from ERNA.

## References

- [1] D.A. Hutcheon, S. Bishop, L. Buchmann, M.L. Chatterjee, A.A. Chen, J.M. D'Auria, S. Engel, D. Gigliotti, U. Greife, D. Hunter, A. Hussein, C.C. Jewett, N. Khan, M. Lamey, A.M. Laird, W. Liu, A. Olin, D. Ottewell, J.G. Rogers, G. Roy, H. Sprenger, C. Wrede, Nucl. Instr. and Meth. A 498 (2003) 190.
- [2] S. Engel, D. Hutcheon, S. Bishop, L. Buchmann, J. Caggiano, M.L. Chatterjee, A.A. Chen, J. D'Auria, D. Gigliotti, U. Greife, D. Hunter, A. Hussein, C.C. Jewett, A.M. Laird, M. Lamey, W. Liu, A. Olin, D. Ottewell, J. Pearson, C. Ruiz, G. Ruprecht, M. Trinczek, C. Vockenhuber, C. Wrede, Nucl. Instr. and Meth. A 553 (2005) 491.
- [3] D. Rogalla, S. Theis, L. Campajola, A. D'Onofrio, L. Gialanella, U. Greife, G. Imbriani, A. Ordine, V. Roca, C. Rolfs, M. Romano, C. Sabbarese, F. Schumann, F. Strieder, F. Terrasi, H.P. Trautvetter, Nucl. Instr. and Meth. A 437 (1999) 266.
- [4] D. Rogalla, F. Terrasi, Prog. Part. Nucl. Phys. 46 (2001) 37.
- [5] D. Rogalla, M. Aliotta, C.A. Barnes, L. Campajola, A. D'Onofrio, L. Gialanella, U. Greife, G. Imbriani, A. Ordine, V. Roca, C. Rolfs, M. Romano, C. Sabbarese, D. Schürmann, F. Schumann, F. Strieder, S. Theis, F. Terrasi, H.P. Trautvetter, Nucl. Phys. A 688 (2001) 549c.
- [6] D. Schürmann, F. Strieder, A. Di Leva, L. Gialanella, N. De Cesare, A. D'Onofrio, G. Imbriani, J. Klug, C. Lubritto, A. Ordine, V. Roca, H. Rocken, C. Rolfs, D. Rogalla, M. Romano, F. Schumann, F. Terrasi, H.P. Trautvetter, Nucl. Instr. and Meth. A 531 (2004) 428.
- [7] W. Liu, G. Imbriani, L. Buchmann, A.A. Chen, J.M. D'Auria, A. D'Onofrio, S. Engel, L. Gialanella, U. Greife, D. Hunter, A. Hussein, D.A. Hutcheon, A. Olin, D. Ottewell, D. Rogalla, J. Rogers, M. Romano, G. Roy, F. Terrasi, Nucl. Instr. and Meth. A 496 (2003) 198.
- [8] W.R. Hannes, Beam current and target density normalization in E952  $^{12}\text{C}(\alpha, \gamma)^{16}\text{O}$  at DRAGON, practicum report, Available from: <<http://dragon.triumf.ca/docs/Wolf-report.pdf>>, 2005.
- [9] T.R. Dillingham, J.R. Macdonald, P. Richard, Phys. Rev. A 24 (1981) 1237.
- [10] J.R. Macdonald, F.W. Martin, Phys. Rev. A 4 (1971) 1965.
- [11] U. Greife, S. Bishop, L. Buchmann, M.L. Chatterjee, A.A. Chen, J.M. D'Auria, S. Engel, D. Gigliotti, D. Hunter, D.A. Hutcheon, A. Hussein, C.C. Jewett, A.M. Laird, M. Lamey, W. Liu, A. Olin, D. Ottewell, J. Rogers, C. Wrede, Nucl. Instr. and Meth. B 217 (2004) 1.
- [12] F.M. White, Fluid Mechanics, fourth ed., WCB/McGraw-Hill, 1999, p. 586.
- [13] J.M. D'Auria, R.E. Azuma, S. Bishop, L. Buchmann, M.L. Chatterjee, A.A. Chen, S. Engel, D. Gigliotti, U. Greife, D. Hunter, A. Hussein, D. Hutcheon, C.C. Jewett, J. Jose, J.D. King, A.M. Laird, M. Lamey, R. Lewis, W. Liu, A. Olin, D. Ottewell, P. Parker, J. Rogers, C. Ruiz, M. Trinczek, C. Wrede, Phys. Rev. C 69 (2004) 065803.
- [14] J.F. Ziegler, J.P. Biersack, U. Littmark, The Stopping and Range of Ions in Matter, Available from: <[www.srim.org](http://www.srim.org)>, 2003.
- [15] G. Schiwietz, P.L. Grande, Nucl. Instr. and Meth. B 175 (2001) 125.
- [16] L. Gialanella, F. Strieder, K. Brand, L. Campajola, A. D'Onofrio, U. Greife, E. Huttel, F. Petrazzuolo, V. Roca, C. Rolfs, M. Romano, M. Romoli, S. Schmidt, W.H. Schulte, F. Terrasi, H.P. Trautvetter, D. Zahnow, Nucl. Instr. and Meth. A 376 (1996) 174.
- [17] C. Vockenhuber, C.O. Ouellet, L. Buchmann, J. Caggiano, A.A. Chen, J.M. D'Auria, D. Frekers, A. Hussein, D.A. Hutcheon, W. Kutschera, K. Jayamanna, D. Ottewell, M. Paul, J. Pearson, C. Ruiz, G. Ruprecht, M. Trinczek, A. Wallner, The  $^{40}\text{Ca}(\alpha, \gamma)^{44}\text{Ti}$  reaction at DRAGON, Nucl. Instr. and Meth. B, submitted for publication.